Research Square

Preprints are preliminary reports that have not undergone peer review.
They should not be considered conclusive, used to inform clinical practice,
or referenced by the media as validated information.

Soil sulfide accumulation and stress mitigation of S. alterniflora by radial oxygen loss and iron enrichment in rhizosphere

Zhenzhen Zhao
Jing Hua
Liyu Cheng
Yuanhang Li
Xueping Chen
Xiaoyan Liu
Chiquan HE (cqhe@shu.edu.cn)
Shanghai University
Daoyuan Wang

Research Article

Keywords: Spartina alterniflora, Scirpus mariqueter, Sulfide, Rhizosphere process, Functional bacteria

Posted Date: June 27th, 2023

DOI: https://doi.org/10.21203/rs.3.rs-3070301/v1

License: This work is licensed under a Creative Commons Attribution 4.0 International License.
Read Full License

Abstract

Background and Aims *Spartina alterniflora* (*S. alterniflora*) is an invasive plant widely distributed in coastal areas of China, and the invasion has caused the accumulation of soil sulfur contents, while sulfide can accumulate to phytotoxic levels. It has been verified that *S. alterniflora* is more tolerant to sulfide than *Scirpus mariqueter* (*S. mariqueter*). Therefore, sulfide may play an important role in invading *S. alterniflora*, but the specific mechanism awaits further investigation.

Methods Through experiments with situ rhizoboxes in the Jiuduansha Wetland, we conducted field investigations to analyze soil sulfur (sulfate and sulfide) contents, iron (Fe(II) and Fe(III)) contents, and physicochemical properties. Lab-scale experiment with high-resolution (HR) diffusive gradients in thin films (DGT) was conducted to investigate the distribution of oxygen, sulfide, and iron concentrations in the microenvironment of two species. Meanwhile, the effect of roots on soil bacterial communities and sulfur cycle-related microorganisms was investigated.

Results The soil sulfur (sulfide and sulfate) contents in *S. alterniflora* were higher than in *S. mariqueter*. In the rhizoboxes of *S. alterniflora*, the contents of soil sulfide were significantly lower in the rhizosphere, while oxygen contents in the rhizosphere were higher than in bulk soil. The iron contents in *S. alterniflora* were significantly higher than in *S. mariqueter*, especially the Fe(III) contents were higher in the rhizosphere.

Conclusion The *S. alterniflora* may gain an advantage in the invasion process by oxidizing the sulfide through radial oxygen loss and by enriching iron to mitigate high concentrations of sulfide in the rhizosphere.

1 Introduction

Coastal wetland, a transition zone between terrestrial and aquatic ecosystems, is an ecological area with high vegetation coverage and periodic flooding of the intertidal zone (Ding et al. 2022). In 1979, *Spartina alterniflora* (*S. alterniflora*) was introduced to China for its ecological role in beach protection and sediment stabilization (Xu et al. 2020). *S. alterniflora* has strong adaptability to climate and was competitive against native species such as *Scirpus mariqueter* (*S. mariqueter*) due to its superior ecophysiological traits (e.g., rapid growth, well-developed belowground structures, and high reproductive capacity) (Xue et al. 2018; Zhang et al. 2019; Chen et al. 2022). The successful invasion of *S. alterniflora* has significantly altered the structure and function of the coastal wetland ecosystem, e.g., affecting soil elemental distribution and transformation (Zuo et al. 2020; Chen et al. 2022).

Sulfur (S) is an essential nutrient for plant growth, and S cycling processes are closely linked to iron, nitrogen, and carbon cycles (Karimian et al. 2018; Jørgensen et al. 2019). The dissimilatory sulfate reduction primarily drives the sulfur cycle of wetland soil sulfide by anaerobic microorganisms (Wu et al. 2021). If the generated sulfide cannot be sufficiently sequestered in the soil by metals, such as iron, the accumulation of reduced S in sediments will cause physiological toxicity stress to the living organisms,

including plants, animals, and microorganisms (Hasler-Sheetal and Holmer 2015; Wu et al. 2022). As a potent phytotoxin, reduced sulfur compounds inhibit energy production by reducing oxidase activity in the mitochondria (Lamers et al. 2013).

S. alterniflora invasion significantly induced shifts in vegetation composition and S cycling processes in coastal wetland ecosystems (Zhou et al. 2009; Xia et al. 2015). Studies have shown that *S. alterniflora* invasion increases total S content by increasing the soil organic matter, which promotes sulfate reduction and sulfide accumulation in soil (Wang et al. 2019; He et al. 2020; Zhao et al. 2022). In addition, *S. alterniflora* invasion promoted sulfur-reducing bacterial (SRB) activities to accelerate sulfur cycling, favoring the invasion of sulfur-tolerant plants (Zheng et al. 2017; Lin et al. 2022). *S. alterniflora*, is known to survive high sulfide concentrations of up to 8 mM, which is much higher than most other salt marsh species (Lamers et al. 2013). Our previous studies have also indicated that the phytotoxicity of sulfides caused more lethal damage to the native species of *S. mariqueter* than to *S. alterniflora* (He et al. 2021a). Therefore, *S. alterniflora* provided more nutrients for its growth and reproduction and simultaneously increased soil sulfur content to exclude the native species with toxicity thresholds.

Roots impact soil microbes through shifting soil nutrient cycling and soil structure, especially in the rhizosphere (Bertin et al. 2003; York et al. 2016; Ma et al. 2018). In tidal wetlands, the soil is typically saturated with water, leading to low oxygen levels and sulfide accumulation. Wetland plants can transfer oxygen to surrounding soils through radial oxygen loss (ROL) (Koop-Jakobsen et al. 2017), which can help counteract the adverse effects of waterlogging and promote microbial growth (Martin et al. 2018). The ROL process can frequently generate ferrous (Fe(II)) and lead to iron precipitation in the rhizosphere (Yang et al. 2014; Khan et al. 2016). Different tidal marsh plants use sulfide to reduce iron in the rhizosphere is connected to the amount of porosity and air channels (aerenchyma) in their roots, which also affects soil sulfur cycling (Luo et al. 2018). These biogeochemical processes in the rhizosphere significantly differed from bulk soil (Lemanceausoils et al. 2009).

Although the element cycling in rhizosphere and bulk soil is well-documented for *S. alterniflora*, only few studies have revealed the micro-scale effect of roots through laboratory scales. Planar optodes visualized the presence of oxygen with a radius up to 1.6 mm around the tips of *Spartina anglica* (Koop-Jakobsen and Wenzhöfer 2015). A multifaceted experiment revealed that the microenvironment created by ROL may enhance both abiotic and bacterial sulfide oxidation and restrict bacteria sulfide production around vulnerable roots, thereby helping seagrasses to colonize sulfide-rich anoxic sediments (Koop-Jakobsen et al. 2017; Martin et al. 2018). To compensate for the difficulty of laboratory experiments and the environmental heterogeneity influenced by multiple factors, we link the field element cycling of situ rhizoboxes in Jiuduansha Wetland with the microscale patterns in rhizosphere of lab-scale experiments.

We sought to elucidate the incidence of roots on the soil sulfur cycle in the rhizosphere and investigate the potential mechanism of *S. alterniflora* to mitigate the high sulfide stress by observing oxygen, sulfide, and iron contents in the rhizosphere. We hypothesized that: (1) *S. alterniflora* can reduce sulfide content by oxidizing the sulfides located near the roots due to radial oxygen loss; (2) the roots of *S. alterniflora*

can alleviate the toxicity of sulfides by enriching iron and combining with free sulfides to form Fe sulfide compounds. This study may be vital to understand the significant impact of sulfide on the rapid invasion of *S. alterniflora*, with potentially significant effects on biogeochemical cycling and plant productivity of coastal wetlands.

2 Material and methods

2.1 Study site and rhizobox design

The study area is located in the Jiuduansha Wetland National Nature Reserve (31°08'~31°15' N, 121°52'~122°03' E) in China, i.e., the section of the Lanmensha River between the north and south troughs outside the estuary of the Yangtze River. The climate of Jiuduansha wetland is subtropical monsoon, with a mean annual temperature of 15–17°C and a mean annual precipitation of about 1200 mm (He et al. 2021b). The dynamic and geomorphological processes of the wetland are profoundly influenced by the distinct interactions between runoff and tidal (semi-diurnal) currents. The maximum and average tidal ranges are 4.62 m and 2.67 m, respectively (Tang et al. 2011). *S. mariqueter* is the dominant species in Jiuduansha Wetland, and the invasion of the *S. alternifora* gradually replace the native *S. mariqueter*.

For the rhizobox experiment, three cuboid-acrylic rhizoboxes (length = 40 cm; width = 15 cm; height = 15 cm) (Fig. 1b) were randomly embedded in each of the *S. alternifora* and *S. mariqueter* communities in Jiuduansha Wetland on May 30th, 2020 (Fig. 1a). The perforated partitions, together with the nylon filter cloth (6.5 μm) are used between the middle compartment (root zone) and the side compartments (bulk soil zone) to block root growth but allowing the soil to exchange material and water, thus dividing the rhizobox into three zones. Eight seedlings were transplanted evenly into the middle compartment. Ten circular holes were drilled on the bottom of the middle compartment to allow material exchange. A piece of nylon filter cloth (6.5 μm) was laid on top of the bulk soil zone to prevent plant growth and entry of macrobenthos (Luo et al. 2018). Soil from each community with roots and large benthic animals was removed, homogenized, and then filled into the rhizoboxes. On November 20, 2020, all rhizoboxes were immediately packed in opaque vacuum bags after being removed from the soil at the ebb tide and kept on ice until they were shipped to the laboratory.

2.2 Soil sampling and preparation

In the laboratory, soil pretreatment was performed in a nitrogen-filled glove box (MIKROUNA, China). To focus on the rhizosphere processes, the potential oxidation layer of the surface soil (about 0–2 cm) was removed. After pulling out the removable partition, sub-samples from each compartment were gradually extruded out, and polypropylene plastic sheets were utilized to separate the bulk soil according to the distance from the root zone (0–1 cm, 1–3 cm, 3–5 cm, 5–10 cm, and 10–17 cm). The soil inside the root zone was carefully cleared of roots and was mixed thoroughly for further analysis. The soil samples for sulfide and iron analyses were stored at -20°C, and soil samples for DNA extraction were stored at -80°C.

The rest of the soil samples were air-dried, passed through a 0.15 mm sieve, and stored for further analyses. Plant litter was removed from soil samples. We named the SA0 for the root zone of *S. alterniflora*, SA1 for 0–1 cm from the root zone, SA2 for 1–3 cm from the root zone, SA3 for 3–5 cm from the root zone, SA4 for 5–10 cm from the root zone, SA5 for 10–17 cm from the root zone, and so on for the rhizoboxes of *S. mariqueter* (Fig. 1b).

2.3 Sample analyses

Each following measurement was conducted with three replicates. The aboveground biomass was determined by drying the plant samples to a constant weight in ovens at 65°C. Soil samples were dried to a constant weight at 105°C to measure soil moisture content. Soil pH was determined using a pH meter (PHS-25, China) at the soil-to-distilled water ratio of 1:2.5 (w/v), and soil salinity was determined using a conductivity meter (Mettler-Toledo, Switzerland) at the soil-to-distilled water ratio of 1:2.5 (w/v). The potassium dichromate oxidation method was used to determine soil organic carbon (SOC) contents. Soil Kjeldahl nitrogen (N) was determined using a Kjeldahl apparatus (Distillation Unit B-324, BUCHI).

The concentrations of Fe(II) and Fe(III) were determined by the 1,10- phenanthroline method (Fernández-de Córdova et al. 1997). Briefly, the HCl-extractable Fe(II) concentration was determined by extraction using 0.5 M hydrochloric acid (HCl). The total HCl- extractable Fe concentration was determined by dissolving with 0.5 M HCl after reducing agent (hydroxylamine hydrochloride) addition. After extraction, all iron species were determined using an enzyme standard (Multiskan FC, Thermo scientific). HCl-extracted Fe(III) was calculated as the difference between the HCl-extracted total Fe and Fe(II). Soil sulfide contents were determined by the methylene blue spectrophotometric method (Niu et al. 2018), and soil sulfate contents were determined by the barium sulfate turbidimetric method (Luo et al. 2018).

2.4 Microbial analyses

Groups of soil DNA were extracted using the FastDNATM Spin Kit for Soil (MP Biomedicals, Europe). The quality of the extracted DNA was checked by 2% agarose gel electrophoresis, and the concentration of the DNA samples was measured by a molecular UV spectrophotometer (Q5000, Quawell, USA). The bacterial DNA in the sample soil was amplified by Majorbio (Shanghai Majorbio Bio-Pharm Technology Co. Ltd, Shanghai, China). Universal primers 341F (5'- CCTAYGGGRBGCASCAG – 3') and 806R (5'-GGACTACHVGGGTWTCTAAT-3') were used to amplify the 16s rDNA genes of the V3–V4 regions. The 16S rDNA gene was sequenced on Illumina Miseq PE 300 by Majorbio.

2.5 Rhizosphere microenvironment analysis with HR-DGT

The plants of the *S. alternifora* and *S. mariqueter* used in the experiment were collected from the Jiuduansha Wetland on 30 July 2020 and transported back to the laboratory in impermeable open boxes, while the corresponding soil was collected from the *S. alternifora* and *S. mariqueter* communities, respectively, dried naturally and then ground for use. The assembled box (26 cm (h) × 14.5 cm (l) × 2 cm (w)) was filled with sieved (< 2 mm) soil and compacted in layers (Martin et al., 2018). A Nuclepore membrane was inserted front the detachable plate to ensure uniform soil distribution during the

deployment of the DGT-binding gel and prevent disturbance to roots and soil when removing the front plate. After saturating the soil for 24 hours, plants were incubated in an artificial climate chamber with 80% relative humidity, 12 hours of light per day, and a temperature of 28°C (day)/20°C (night) before being transplanted into prepared boxes at a 45 ° angle with the detachable front plate downwards to facilitate root growth alongside the Nuclepore membrane. Tinfoil was wrapped around the box to prevent the effect of light on microorganisms. Subsequent experiments were started after 3 to 4 weeks of culture when visible roots could be observed.

The HR-DGT techniques were used to determine the soil sulfide contents and soluble iron contents of the rhizosphere (Fang et al. 2018). Specifically, AgI sorbent gels, made of polyacrylamide hydrogels impregnated with silver iodide, formed black silver sulfide precipitates upon reacting with dissolved sulfide, which was then quantified using computer imaging analysis. The ultra-thin SPR-IDA adsorbent gel consists of a fine iminodiacetate adsorbent (SPR-IDA) of about 0.2 μm, which adsorbs divalent cations and is applied here with a primary focus on iron concentration. Laser exfoliation-inductively coupled plasma mass spectrometry (LA-ICPMS) was used to analyze the SPR-IDA adsorbent gel (Warnken et al. 2004) after the sorbent was initially dried overnight and then dried for 8 hours at 60°C in a dry gelator (5 Model 583, Biorad, Hercules, CA). The dried samples and standards were ablated to aerosols using a laser ablation system (UP-213, New Wave Research, Fremont, CA) and transported via a helium carrier to the LA-ICPMS (7700, Agilent Technologies, Santa Clara, CA) for elemental analysis. The concentration of the target element was obtained by calculating the ratio of the target element to the ^{13}C signal value, and the data were stitched together using Python 3.9 to restore the concentration in the two-dimensional plane of the adsorbed gel.

2.6 Data analyses

For the physicochemical factors of the soils of both *S. alternifora* and *S. mariqueter*, the mean and standard deviation (SD) were calculated for triplicate samples of each plant by SPSS 25.0 software. One-way ANOVA and Tukey's test were applied to test for significant differences among the different factors. The data were plotted using the software Origin 8.5. Structural equation modeling (SEM) was constructed using the software IBM SPSS Amos 26 (Amos Development Corporation, Meadville, PA, USA). The theoretical SEM model was first constructed between independent and dependent variables based on previous studies and a priori knowledge using AMOS software. Distance from the root zone was used as an exogenous variable, and soil physical properties (including water contents and pH) and soil chemical properties (including organic carbon, Fe(II) and Fe(III), sulfate, and sulfide contents) were used as endogenous variables. Then the final model was further optimized based on the arithmetic results of the theoretical model. In the SEM model, chi-square tests ($P > 0.05$) indicated a good fit of the model to the data.

For 16s rDNA sequencing data, three indices of alpha diversity, including ACE, Chao1, and Shanno indices, were calculated using MajorBio's online cloud platform (https://cloud.majorbio.com) to reflect the diversity and abundance of bacterial communities. Multidimensional Principal Component Analysis

(Multi-way PCA) was used to analyze the composition of microbial communities among different soil samples. A redundancy analysis (RDA) of the soil bacterial communities of two plants at different distances from the root zone concerning soil environmental factors was performed after screening for environmental factors by variance inflation factor analysis (VIF). The selection of representative sulfur reducing bacteria (SRB) and sulfur oxidizing bacteria (SOB) was made based on the relevant literature (Karimian et al. 2018; Niu et al. 2018). Statistical differences in the relative abundance of dominant bacteria (phylum level) in the rhizosphere of *S. alterniflora* and *S. mariqueter* were analyzed using the Wilcoxon rank-sum test on MajorBio's online cloud platform. FAPROTAX (Functional annotation of prokaryotic taxa) performs functional annotation and prediction of biogeochemical cycles in environmental samples (Louca et al. 2016). The annotated OTU information was matched with information on sulfur redox and iron redox species in the FAPROTAX database (www.zoology.ubc.ca/louca/FAPROTAX) via Python to output the predictions of the functions.

3 Results

3.1 Soil sulfur and Fe contents in rhizoboxes

Sulfide and sulfate contents in soil were higher in *S. alternifora* than in *S. mariqueter* (Table 1). The soil sulfide content in SA3 (1–3 cm from root zone) was significantly higher than that in SA0 (root zone), and the highest soil sulfate content of *S. alternifora* was in SA0. There were no significant differences in soil sulfate contents in groups of *S. mariqueter*, as well as the soil sulfide contents.

Soil Fe(II) and Fe(III) of *S. alternifora* were higher than those in *S. mariqueter* (Table 1). There were no significant differences in soil Fe(II) contents of *S. alternifora*, while soil Fe(III) content in SA0 was significantly higher than bulk soil zone. Meanwhile, the further away from the root zone, the lower soil Fe(III) contents were. In *S. mariqueter*, there was no significant difference in soil Fe(II) and Fe(III) contents in each zone, but the soil Fe(II) contents were much higher than those of Fe(III). The highest total Fe content of *S. alternifora* was in SA0, much higher than in the bulk soil zone.

Table 1
Contents of soil Fe(II) and Fe(III) in different zones of rhizoboxes; contents of soil sulfate and sulfide in different zones of rhizoboxes (SA, *S. alterniflora*; SM, *S. mariqueter*). Different letters indicate concentrations of significant differences ($p < 0.05$) between six groups of each rhizobox.

Physicochemical properties	Plant	Root zone	0 ~ 1 cm	1 ~ 3 cm	3 ~ 5 cm	5 ~ 10 cm	10 ~ 17 cm
Fe(II) (mg/g)	SA	3.11 ± 0.18 ns	2.44 ± 0.41 ns	2.63 ± 0.27 ns	3.13 ± 0.20 ns	2.81 ± 0.48 ns	3.13 ± 0.33 ns
	SM	0.91 ± 0.13 ns	1.08 ± 0.09 ns	1.00 ± 0.20 ns	1.15 ± 0.14 ns	1.17 ± 0.16 ns	1.28 ± 0.01 ns
Fe(III) (mg/g)	SA	2.69 ± 0.08 a	2.17 ± 0.34 ab	1.98 ± 0.11 b	1.69 ± 0.24 b	1.84 ± 0.06 b	1.70 ± 0.30 b
	SM	0.03 ± 0.01 ns	0.01 ± 0.01 ns	0.01 ± 0.01ns	0.01 ± 0.00 ns	0.00 ± 0.00 ns	0.03 ± 0.02 ns
Sulfide (mg/kg)	SA	37.68 ± 8.93 b	48.83 ± 26.63 ab	92.85 ± 18.24 a	38.04 ± 13.93 b	44.84 ± 9.43 b	34.15 ± 16.18 b
	SM	20.52 ± 1.51 ns	22.49 ± 5.13 ns	23.29 ± 4.32 ns	20.61 ± 3.03 ns	17.55 ± 0.91 ns	20.14 ± 0.92 ns
Sulfate (mg/kg)	SA	329.17 ± 53.16 a	164.17 ± 21.86 b	218.33 ± 23.03 ab	200.00 ± 17.74 b	259.17 ± 9.61 ab	237.50 ± 5.20 ab
	SM	166.67 ± 25.34 ns	114.58 ± 16.37 ns	119.79 ± 15.76 ns	117.71 ± 12.28 ns	120.83 ± 20.91 ns	169.79 ± 22.27 ns

3.2 Structural equation modeling (SEM) of soil properties in rhizoboxes

The differences in soil properties including soil pH, water content, soil nitrogen, and carbon are shown in Table 2. The plant biomass of *S. alterniflora* (33.67 ± 4.62 g) was 4 times higher than that of *S. mariqueter* (7.67 ± 2.62 g). Soil pH was lower in the root zone of *S. alterniflora* than in the bulk soil zone, while there were no significant differences in *S. mariqueter* (Table 2). There was higher soil water content in the root zone of both species. In *S. alterniflora*, both nitrogen and organic carbon contents of the root zone were 2 times higher than the bulk soil zone, with no significant differences in *S. mariqueter*.

Table 2
Physicochemical properties in soils of different distances from the root zone (SA, *S. alterniflora*; SM, *S. mariqueter*). The data were expressed as means ± SDs. Different letters indicate significant differences between six groups of each rhizobox at a $p < 0.05$ level.

Physicochemical properties	Plant	Root zone	0 ~ 1 cm	1 ~ 3 cm	3 ~ 5 cm	5 ~ 10 cm	10 ~ 17 cm
pH	SA	8.42 ± 0.04 c	8.78 ± 0.07 b	8.81 ± 0.06 b	8.85 ± 0.05 b	8.85 ± 0.02 b	9.00 ± 0.01 a
	SM	8.73 ± 0.09 ns	8.70 ± 0.07 ns	8.69 ± 0.06 ns	8.75 ± 0.08 ns	8.80 ± 0.08 ns	8.77 ± 0.08 ns
water content (%)	SA	33.51 ± 1.05 a	29.07 ± 1.17 b	28.12 ± 0.31 b	27.22 ± 0.46 b	27.82 ± 3.68 b	28.18 ± 1.16 b
	SM	27.15 ± 1.03 a	24.07 ± 1.18 b	24.80 ± 0.50 b	24.06 ± 0.52 b	24.34 ± 0.33 b	25.29 ± 0.69 b
SOC (mg/g)	SA	11.54 ± 0.80 a	5.48 ± 0.57 b	5.67 ± 0.44 b	5.00 ± 0.20 b	4.93 ± 0.22 b	4.53 ± 0.34 b
	SM	4.48 ± 0.23 ns	4.50 ± 0.38 ns	4.69 ± 0.54 ns	4.74 ± 1.01 ns	3.78 ± 0.87 ns	4.52 ± 0.37 ns
N (mg/g)	SA	1.21 ± 0.09 a	0.72 ± 0.12 b	0.64 ± 0.05 bc	0.58 ± 0.03 bc	0.56 ± 0.00 bc	0.51 ± 0.05 c
	SM	0.30 ± 0.02 ns	0.32 ± 0.02 ns	0.31 ± 0.00 ns	0.32 ± 0.00 ns	0.28 ± 0.00 ns	0.30 ± 0.03 ns

The structural equation modeling (SEM) of soil properties showed significant differences in the correlation between soil physicochemical properties of *S. alterniflora* and *S. mariqueter* (Fig. 2). In *S. alterniflora*, the distance from the root zone was a direct factor in regulating sulfate (path coefficient = 0.87), soil water content was negatively correlated with soil sulfide contents (path coefficient = − 0.92) and soil Fe(II) content was positively correlated with soil sulfide contents (path coefficient = 0.55). Furthermore, Pearson correlation analysis revealed a significant positive correlation between soil sulfate contents and soil organic carbon contents ($p < 0.05$) and a significant negative correlation with soil pH (Fig. S 1).

In *S. mariqueter*, soil organic carbon contents were positively correlated with sulfide contents (path coefficient = 0.51), with a positive correlation between soil water contents and sulfate contents (path coefficient = 0.45). Pearson correlation analysis showed that there was a significant positive correlation between soil Fe(III) contents and soil sulfate contents ($p < 0.05$) (Fig. S 1). Taken together, these two statistical analyses showed that the roots of *S. alterniflora* modify the sulfide and sulfate contents by regulating the physicochemical properties of the soil, which was not present in *S. mariqueter*.

3.3 Soil microbial community composition

The abundance of *Desulfobacterota* in *S. alterniflora* was 2.7 times higher than in *S. mariqueter*, with the opposite results observed in the root zones of *S. alterniflora* and *S. mariqueter* (Fig. S 2). The abundance of microbial sulfur function bacteria in the soil of *S. alterniflora* was higher than that of *S. mariqueter*, and the microbial sulfur redox function bacteria in the root zone of both plant communities were lower than the respective bulk soil zones (Fig. 3). The relative abundance of the dominant sulfur reducing bacteria (SRB), such as *Desulfobulbaceae*, *Sva0081_sediement_group*, and *Thermodesulfovibrionia* in the rhizoboxes of *S. alterniflora* were higher than those in the *S. mariqueter* (Fig. S 3), with *Desulfobulbaceae* was 2.7-fold of *S. mariqueter*. The Fe redox function bacteria in the soil of *S. alterniflora* were more active than *S. mariqueter* (Fig. 4). The relative abundance of the microbial iron reduction bacteria (FeRB) in the root zone (SM0) of *S. alterniflora* was lower than the bulk soil zone. The closer to the root zone of *S. mariqueter*, the fewer the microbial iron oxidizing bacteria (FeOB) were. The relative abundance of the FeRB *Geothermobacter* and the FeOB *Rhodobacteraceae* was significantly higher in *S. alterniflora* than in *S. mariqueter* (Fig. S 4). In the soil of *S. alterniflora*, the dominant FeRB (*Geothermobacter* and *Anaeromyxobacter*) and dominant FeOB (*Rhodobacteraceae* and *Hyphomicrobium*) were higher in the root zone.

3.4 HR-DGT in the rhizosphere

The dissolved oxygen concentration near the roots of *S. alterniflora* is 1–2 mg/L (Fig. 5a), higher than the oxygen concentration in the bulk soil at the same height. This indicates that the aerenchyma of *S. alterniflora* can transport the absorbed oxygen from the aboveground to the anaerobic soil. There was still 1.5-2 mg/L dissolved oxygen initially in the soil near the roots of *S. mariqueter* (Fig. 5b1), which was caused by the absorption of dissolved oxygen in the added water during the physiological and biochemical activities of the roots. After a period of static time, the dissolved oxygen concentration in the water decreased to 0 mg/L and no change in the dissolved oxygen concentration near the roots of *S. mariqueter* (Fig. 5b2), indicating that the roots of *S. mariqueter* did not secrete oxygen in the rhizosphere.

The iron concentrations in the soil of *S. alterniflora* (Fig. 6a) were much higher than those of *S. mariqueter* (Fig. 6c), which were also consistent with the results of the situ rhizobox experiments in 3.1. It was worth noting that the high concentrations of Fe in the root system of *S. alterniflora*, whereas no roots-related variation near the roots of *S. mariqueter*. Sulfide concentrations near the rhizosphere of *S. alterniflora* were significantly lower than in other areas (Fig. 6b). The high sulfide concentrations in parts of the area beneath the roots of *S. alterniflora* were consistent with the spot aggregation areas. No change in sulfide concentration was observed near any of the roots of *S. mariqueter* (Fig. 6d).

4 Discussion

ROL in *S. alterniflora* corresponded to a decrease in sulfide contents in the rhizosphere, indicating that the ROL served as a protective barrier against sulfide intrusion when the plant was fully anaerobic. Sulfide exhibit phytotoxicity in rapid redox reactions with sulfate under tidal conditions in coastal wetlands (Lamers et al. 2013). The difference between the ROL of the *S. alterniflora*, and no oxygen release

observed near the roots of the *S. mariqueter* (Fig. 5), may have resulted in different strategies for the two plants under the same adversity (Manzur et al. 2014). The presence of well-developed aerenchyma within the roots of *S. alterniflora* provides an oxygen transfer channel for root respiration in anaerobic soil (Koop-Jakobsen et al. 2017). ROL not only provided a favorable oxidative state microenvironment for aerobic microorganisms (Bai et al. 2023) but also changed the morphology and bio effectiveness of elements in the microenvironment of rhizosphere (Peralta Ogorek et al. 2023), forming ferromanganese oxide plaque on the surface of the root and reducing toxic substances and heavy metals in the soil (Ma et al. 2018). The roots of *S. alterniflora* oxidized sulfide in the root zone to protect itself (Table 1), while the high content of sulfide in the bulk soil continues to be harmful to other species with lower toxicity threshold (Lamers et al. 2013; León et al. 2023; Peralta Ogorek et al. 2023).

Our results confirmed that *S. alterniflora* may achieve mitigation of high sulfide stress through iron enrichment near the roots and forming insoluble iron sulfide metals. The roots of *S. alterniflora* may alter soil Fe contents by regulating the activity of Fe redox bacteria (Fig. 4) (Q. Zhang, Yan, and Li 2021), enriching soil Fe near the roots for survival, and influencing soil sulfur morphology and contents (Table 1) (Beck et al. 2008; Ma et al. 2018). The oxidizing microenvironment created by ROL in the rhizosphere favors the accumulation of FeOB (Fig. 4) (Kaplan et al. 2016), facilitating the conversion of Fe(II) to Fe(III) and the deposition of iron minerals on the root surface (Fig. 4), while the roots contribute to the Fe transfer from bulk soil to the rhizosphere, which was the ideal habitat for FeRB (Xiao et al. 2021). Iron reduction is one of the major geochemical changes following the inundation of wetland sediment (Karimian et al. 2018). As a dominant pathway in iron reduction, sulfidation accelerating Fe(III) to be abiotically reduced by free sulfide and produce ferrous sulfide (FeS), which is prone to transforming into the more thermodynamically stable pyrite (e.g., FeS_2) if further sulfide is available (Hansel et al. 2015; Fan et al. 2023).

We found that the roots alter the sulfur cycle by affecting the distribution of Fe and oxygen and further play a significant role in the invasion of the *S. alterniflora* community into the *S. mariqueter* community. The aerenchyma of *S. alterniflora* reduced the sulfide content by transporting the oxygen to the anaerobic zone near the roots (Fig. 5) and enriching the iron in the rhizosphere (Fig. 6) that can combine with free sulfide to form stable iron sulfides further reducing the sulfide content. Thus, the roots of *S. alterniflora* may form a self-protective microenvironment to alleviate the toxicity of high sulfide levels in anaerobic and high-sulfur environments, consistent with previous research (Manzur et al. 2014; Hansel et al. 2015; León et al. 2023). The abundant biomass that provides sufficient nutrients for growth further promotes the rapid reproduction of *S. alterniflora*, accelerating the occupation of ecological niches and is conducive to colonization and expansion in the invasion process.

5 Conclusion

Our results suggest a potential invasive mechanism that *S. alterniflora* can increase the sulfide contents of wetland soils and mitigate high sulfide stress. First, the aerenchyma of *S. alterniflora* reduced sulfide concentrations by transferring oxygen absorbed above ground to the oxygen-deficient rhizosphere, where

the oxygen oxidizes sulfide and decreases the sulfide contents. Second, iron enriched in the rhizosphere of *S. alterniflora* can combine with free sulfide and FeS to form more iron sulfide (e.g., pyrite). This reaction helps in reducing sulfide concentration near the roots and forming iron plaque as a barrier to prevent the toxic effect of sulfide on the roots, thus creating a protective environment to alleviate high sulfide stress. In summary, ROL and iron enrichment of *S. alterniflora* roots function in a combination of chemical and biological pathways in the rhizosphere to provide a means for survival in the environment with high sulfide content. For future work, intensive studies on the iron plaque formation around the roots of *S. alterniflora* and its role in mitigating the high sulfide stress in the rhizosphere are needed.

Abbreviations

ROL
radial oxygen loss
SA
Spartina alterniflora
SM
Scirpus mariqueter
S
sulfur
SRB
sulfur reducing bacteria
SOB
sulfur oxidizing bacteria
FeRB
iron reducing bacteria
FeOB
iron oxidizing bacteria

Declarations

Acknowledgements

This study was financially supported by the Natural Science Foundation (41971055). Great thanks to the group who provided invaluable support while the samples were collected.

Funding: This study was financially supported by the Natural Science Foundation (41971055).

Competing Interests: The authors declare that they have no known competing financial interests or personal relationships that could have appeared to influence the work reported in this paper.

Author Contributions: Zhenzhen Zhao: Conceptualization, Software, Methodology. Jing Hua: Data curation, Writing- Original draft preparation. Liyu Cheng: Investigation, Resources. Yuanhang Li:

Investigation, Visualization. Xueping Chen: Writing- Reviewing and Editing, Methodology. FeifeiWang: Investigation. Xiaoyan Liu: Investigation. Chiquan He: Supervision, Funding acquisition, Project administration. Daoyuan Wang: Conceptualization, Writing- Reviewing and Editing, Visualization.

Data Availability: The datasets generated during and/or analysed during the current study are available from the corresponding author on reasonable request.

References

1. Bai S, Chen J, Guo M et al (2023) Vertical-scale spatial influence of radial oxygen loss on rhizosphere microbial community in constructed wetland. Environ Int 171:107690. https://doi.org/10.1016/J.ENVINT.2022.107690
2. Beck M, Dellwig O, Holstein JM et al (2008) Sulphate, dissolved organic carbon, nutrients and terminal metabolic products in deep pore waters of an intertidal flat. Biogeochemistry 89:221–238. https://doi.org/10.1007/s10533-008-9215-6
3. Bertin C, Yang X, Weston LA (2003) The role of root exudates and allelochemicals in the rhizosphere. Plant Soil 256:67–83. https://doi.org/10.1023/A:1026290508166/METRICS
4. Chen S, Gao D, Zhang J et al (2022) Invasive Spartina alterniflora accelerates soil gross nitrogen transformations to optimize its nitrogen acquisition in an estuarine and coastal wetland of China. Soil Biol Biochem 174:108835. https://doi.org/10.1016/j.soilbio.2022.108835
5. Ding W, Xie W, Xu J et al (2022) Effects of methyl halide flux characteristics following Spartina alterniflora invasion in a seaward direction in a temperate salt marsh, China. Sci Total Environ 847:157607. https://doi.org/10.1016/J.SCITOTENV.2022.157607
6. Fan Y, Sun S, He S (2023) Iron plaque formation and its effect on key elements cycling in constructed wetlands: Functions and outlooks. Water Res 235:119837. https://doi.org/10.1016/J.WATRES.2023.119837
7. Fang W, Williams PN, Fang X et al (2018) Field-Scale Heterogeneity and Geochemical Regulation of Arsenic, Iron, Lead, and Sulfur Bioavailability in Paddy Soil. Environ Sci Technol 52:12098–12107. https://doi.org/10.1021/ACS.EST.8B01947
8. Fernández-de Córdova ML, Ruíz-Medina A, Molina-Díaz A (1997) Solid-phase spectrophotometric microdetermination of iron with ascorbic acid and ferrozine. Fresenius' J Anal Chem 1997 357(1 357):44–49. https://doi.org/10.1007/S002160050108
9. Hansel CM, Lentini CJ, Tang Y et al (2015) Dominance of sulfur-fueled iron oxide reduction in low-sulfate freshwater sediments. ISME J 9:2400–2412. https://doi.org/10.1038/ismej.2015.50
10. Hasler-Sheetal H, Holmer M (2015) Sulfide intrusion and detoxification in the seagrass zostera marina. PLoS ONE 10. https://doi.org/10.1371/JOURNAL.PONE.0129136
11. He C, Cheng L, Wang D et al (2021a) Spartina alterniflora raised soil sulfide content by regulating sulfur cycle-associated bacteria in the Jiuduansha Wetland of China. Plant Soil. https://doi.org/10.1007/s11104-021-05154-x

12. He C, Wang X, Wang D et al (2021b) Impact of Spartina alterniflora invasion on soil bacterial community and associated greenhouse gas emission in the Jiuduansha wetland of China. Appl Soil Ecol 168. https://doi.org/10.1016/j.apsoil.2021.104168
13. He T, Sun Z, Hu X et al (2020) Effects of Spartina alterniflora invasion on spatial and temporal variations of total sulfur and inorganic sulfur fractions in sediments of salt marsh in the Min River estuary, southeast China. Ecol Indic 113:106253. https://doi.org/10.1016/J.ECOLIND.2020.106253
14. Jørgensen BB, Findlay AJ, Pellerin A (2019) The Biogeochemical Sulfur Cycle of Marine Sediments. Front Microbiol 10:1–27. https://doi.org/10.3389/fmicb.2019.00849
15. Kaplan DI, Kukkadapu R, Seaman JC et al (2016) Iron mineralogy and uranium-binding environment in the rhizosphere of a wetland soil. Sci Total Environ 569–570:53–64. https://doi.org/10.1016/J.SCITOTENV.2016.06.120
16. Karimian N, Johnston SG, Burton ED (2018) Iron and sulfur cycling in acid sulfate soil wetlands under dynamic redox conditions: A review. Chemosphere 197:803–816. https://doi.org/10.1016/j.chemosphere.2018.01.096
17. Khan N, Seshadri B, Bolan N et al (2016) Root Iron Plaque on Wetland Plants as a Dynamic Pool of Nutrients and Contaminants. Adv Agron 138:1–96. https://doi.org/10.1016/BS.AGRON.2016.04.002
18. King GM, Garey MA (1999) Ferric iron reduction by bacteria associated with the roots of freshwater and marine macrophytes. Appl Environ Microbiol 65:4393–4398. https://doi.org/10.1128/AEM.65.10.4393-4398.1999
19. Koop-Jakobsen K, Fischer J, Wenzhöfer F (2017) Survey of sediment oxygenation in rhizospheres of the saltmarsh grass - Spartina anglica. Sci Total Environ 589:191–199. https://doi.org/10.1016/J.SCITOTENV.2017.02.147
20. Koop-Jakobsen K, Wenzhöfer F (2015) The Dynamics of Plant-Mediated Sediment Oxygenation in Spartina anglica Rhizospheres—a Planar Optode Study. Estuaries Coasts 38:951–963. https://doi.org/10.1007/S12237-014-9861-Y/TABLES/1
21. Lamers LPM, Govers LL, Janssen ICJM et al (2013) Sulfide as a soil phytotoxin-a review. Front Plant Sci 4:1–14. https://doi.org/10.3389/fpls.2013.00268
22. Lemanceausoils P, Bauer P, Kraemer S, Briat JF (2009) Iron dynamics in the rhizosphere as a case study for analyzing interactions between soils, plants and microbes. Plant Soil 321:513–535. https://doi.org/10.1007/S11104-009-0039-5/TABLES/3
23. León L, Ogorek P, Takahashi H et al (2023) The barrier to radial oxygen loss protects roots against hydrogen sulphide intrusion and its toxic effect. New Phytol 238:1825–1837. https://doi.org/10.1111/NPH.18883
24. Lin Y, Hu HW, Yang P, Ye G (2022) Spartina alterniflora invasion has a greater impact than non-native species, Phragmites australis and Kandelia obovata, on the bacterial community assemblages in an estuarine wetland. Sci Total Environ 822:153517. https://doi.org/10.1016/J.SCITOTENV.2022.153517

25. Louca S, Parfrey LW, Doebeli M (2016) Decoupling function and taxonomy in the global ocean microbiome. Science (1979) 353:1272–1277. https://doi.org/10.1126/SCIENCE.AAF4507/SUPPL_FILE/LOUCA.SM.PDF
26. Luo M, Liu Y, Huang J et al (2018) Rhizosphere processes induce changes in dissimilatory iron reduction in a tidal marsh soil: a rhizobox study. Plant Soil 433:83–100. https://doi.org/10.1007/s11104-018-3827-y
27. Ma X, Zarebanadkouki M, Kuzyakov Y, Blagodatskaya E (2018) Spatial patterns of enzyme activities in the rhizosphere: Effects of root hairs and root radius. Soil Biol Biochem 118:69–78. https://doi.org/10.1016/j.soilbio.2017.12.009
28. Manzur ME, Grimoldi AA, Insausti P et al (2014) Radial oxygen loss and physical barriers in relation to root tissue age in species with different types of aerenchyma. Funct Plant Biol 42:9–17. https://doi.org/10.1071/FP14078
29. Martin BC, Bougoure J, Ryan MH et al (2018) Oxygen loss from seagrass roots coincides with colonisation of sulphide-oxidising cable bacteria and reduces sulphide stress. The ISME Journal 2018 13:3 13:707–719. https://doi.org/10.1038/s41396-018-0308-5
30. Niu Z, Pan H, Guo X, pan et al (2018) Sulphate-reducing bacteria (SRB) in the Yangtze Estuary sediments: Abundance, distribution and implications for the bioavailibility of metals. Sci Total Environ 634:296–304. https://doi.org/10.1016/J.SCITOTENV.2018.03.345
31. Peralta Ogorek LL, Takahashi H, Nakazono M, Pedersen O (2023) The barrier to radial oxygen loss protects roots against hydrogen sulphide intrusion and its toxic effect. New Phytol. https://doi.org/10.1111/NPH.18883
32. Tang Y, Wang L, Jia J wei, et al (2011) Response of soil microbial community in Jiuduansha wetland to different successional stages and its implications for soil microbial respiration and carbon turnover. Soil Biol Biochem 43:638–646. https://doi.org/10.1016/J.SOILBIO.2010.11.035
33. Wang Z, Zhang H, He C et al (2019) Spatiotemporal variability in soil sulfur storage is changed by exotic Spartina alterniflora in the Jiuduansha Wetland, China. Ecol Eng 133:160–166. https://doi.org/10.1016/j.ecoleng.2019.04.014
34. Warnken KW, Zhang H, Davison W (2004) Performance characteristics of suspended particulate reagent-iminodiacetate as a binding agent for diffusive gradients in thin films. Anal Chim Acta 508:41–51. https://doi.org/10.1016/J.ACA.2003.11.051
35. Wu B, Liu F, Fang W et al (2021) Microbial sulfur metabolism and environmental implications. Sci Total Environ 778:146085. https://doi.org/10.1016/J.SCITOTENV.2021.146085
36. Wu Y, Leng Z, Li J et al (2022) Increased fluctuation of sulfur alleviates cadmium toxicity and exacerbates the expansion of Spartina alterniflora in coastal wetlands. Environ Pollut 292:118399. https://doi.org/10.1016/J.ENVPOL.2021.118399
37. Xia L, Yang W, Zhao H et al (2015) High Soil Sulfur Promotes Invasion of Exotic Spartina alterniflora into Native Phragmites australis Marsh. Clean (Weinh) 43:1666–1671. https://doi.org/10.1002/clen.201300883

38. Xiao S, Luo M, Liu Y et al (2021) Rhizosphere effect and its associated soil-microbe interactions drive iron fraction dynamics in tidal wetland soils. Sci Total Environ 756:144056. https://doi.org/10.1016/J.SCITOTENV.2020.144056
39. Xu X, Liu H, Liu Y et al (2020) Human eutrophication drives biogeographic salt marsh productivity patterns in China. Ecol Appl 30. https://doi.org/10.1002/eap.2045
40. Xue L, Li X, Zhang Q et al (2018) Elevated salinity and inundation will facilitate the spread of invasive Spartina alterniflora in the Yangtze River Estuary, China. J Exp Mar Biol Ecol 506:144–154. https://doi.org/10.1016/J.JEMBE.2018.06.008
41. Yang J, Tam NFY, Ye Z (2014) Root porosity, radial oxygen loss and iron plaque on roots of wetland plants in relation to zinc tolerance and accumulation. Plant Soil 374:815–828. https://doi.org/10.1007/S11104-013-1922-7/TABLES/4
42. York LM, Carminati A, Mooney SJ et al (2016) The holistic rhizosphere: Integrating zones, processes, and semantics in the soil influenced by roots. J Exp Bot 67:3629–3643
43. Zhang G, Bai J, Jia J et al (2019) Shifts of soil microbial community composition along a short-term invasion chronosequence of Spartina alterniflora in a Chinese estuary. Sci Total Environ 657:222–233. https://doi.org/10.1016/J.SCITOTENV.2018.12.061
44. Zhang Q, Yan Z, Li X (2021) Iron plaque formation and rhizosphere iron bacteria in Spartina alterniflora and Phragmites australis on the redoxcline of tidal flat in the Yangtze River Estuary. Geoderma 392:115000. https://doi.org/10.1016/J.GEODERMA.2021.115000
45. Zhao Z, Cheng L, He C et al (2022) Spartina alterniflora Invaded Coastal Wetlands by Raising Soil Sulfur Contents: A Meta-Analysis. Water (Basel) 14:1633. https://doi.org/10.3390/w14101633
46. Zheng Y, Bu NS, Long XE et al (2017) Sulfate reducer and sulfur oxidizer respond differentially to the invasion of Spartina alterniflora in estuarine salt marsh of China. Ecol Eng 99:182–190. https://doi.org/10.1016/J.ECOLENG.2016.11.031
47. Zhou C, An S, Deng Z et al (2009) Sulfur storage changed by exotic Spartina alterniflora in coastal saltmarshes of China. Ecol Eng 35:536–543. https://doi.org/10.1016/J.ECOLENG.2008.01.004
48. Zuo X, Cui L, Li W et al (2020) Spartina alterniflora Leaf and Soil Eco-Stoichiometry in the Yancheng Coastal Wetland. Plants (Basel) 10:1–11. https://doi.org/10.3390/PLANTS10010013

Figures

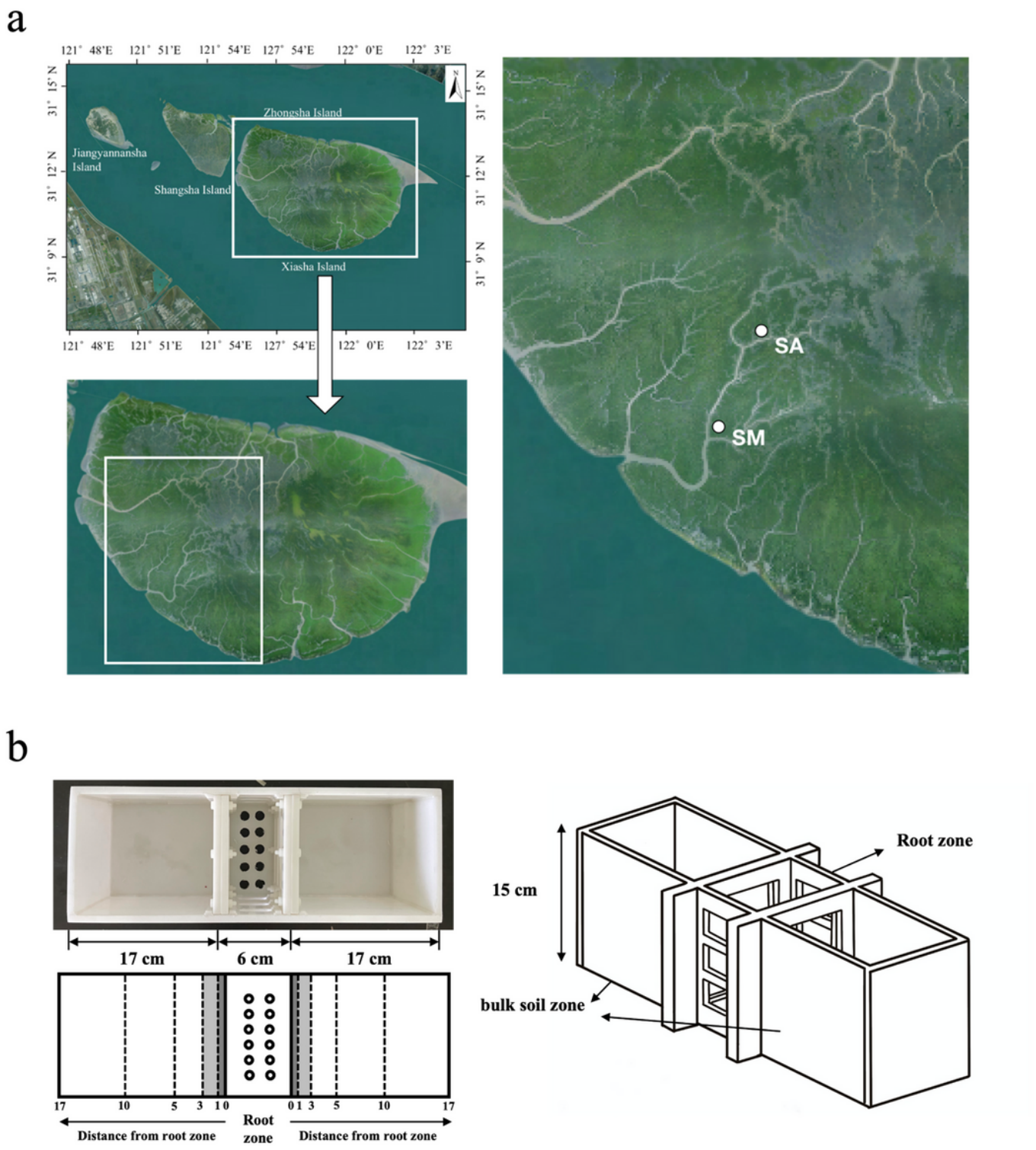


Figure 1

The location of situ rhizoboxes experiments (SA, *S. alterniflora*; SM, *S. mariqueter*) (a); and the schematic diagram of the rhizoboxes (b).

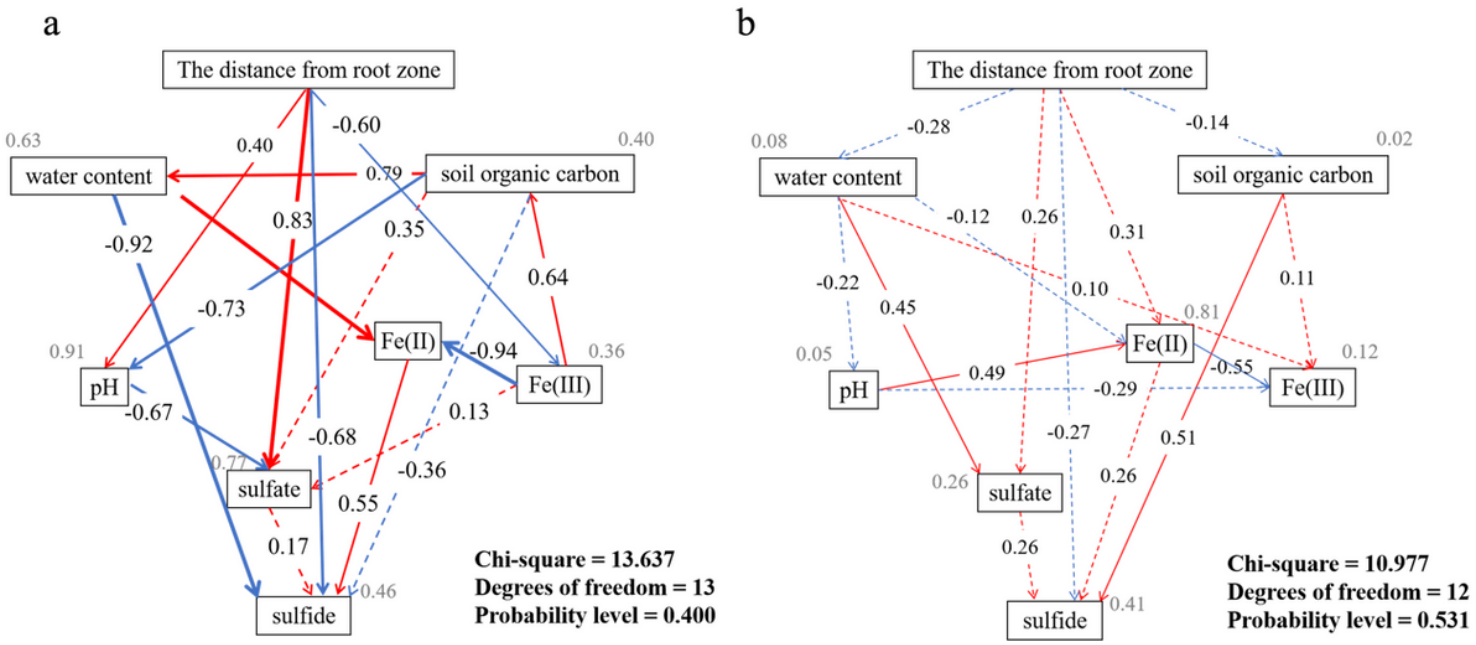


Figure 2

Structural equation model (SEM) of soil sulfide contents regulated by the roots of *S. alterniflora* (a) and *S. mariqueter*(b)

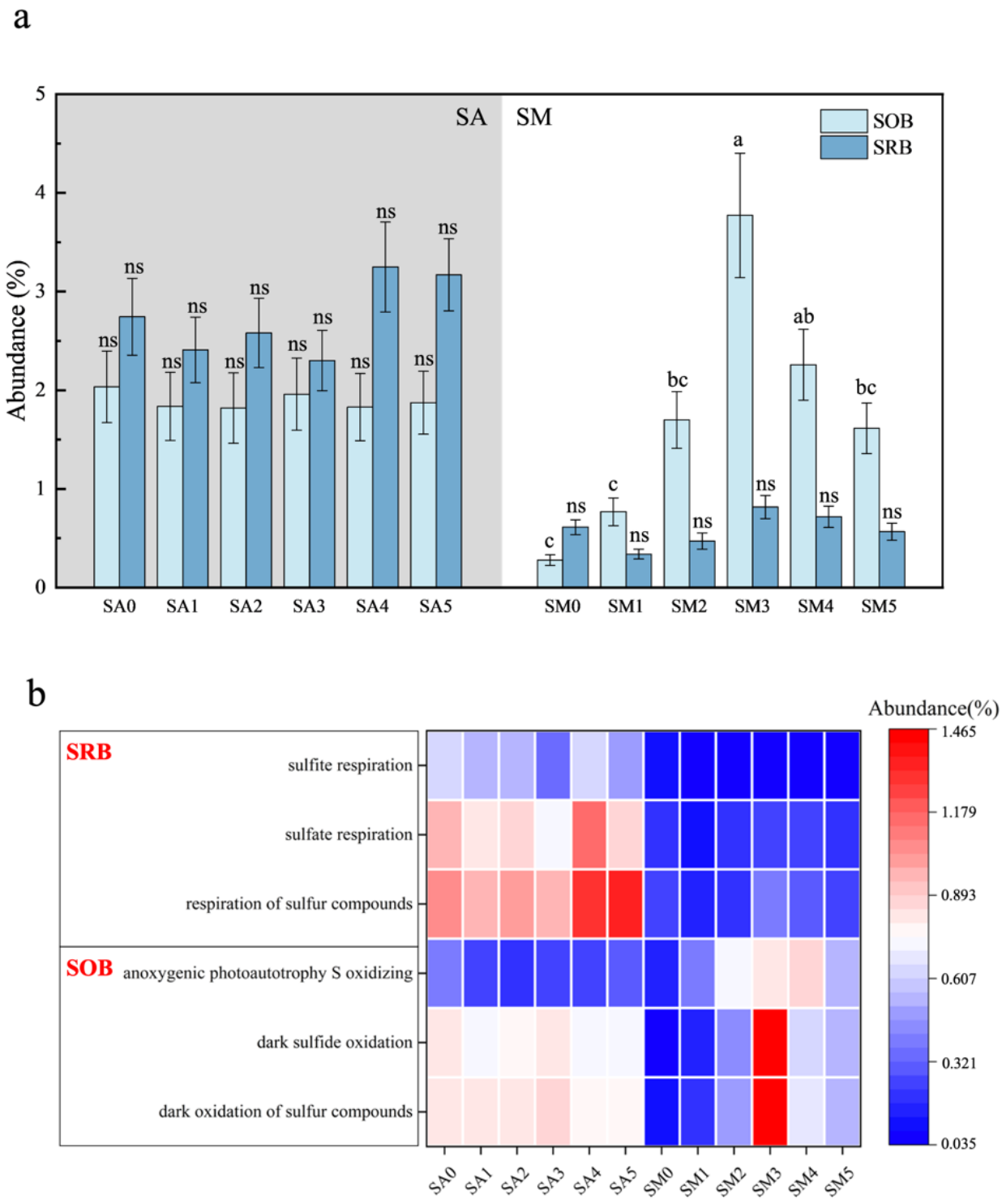


Figure 3

The relative abundance of the microbial sulfur redox function (a) and the main microbial sulfur oxidation and reduction function (b) in the soil of different distances from the root zone in the rhizoboxes of SA (*S. alterniflora*) and SM (*S. mariqueter*) predicted by the FAPROTAX database (SA0 for the root zone of *S. alterniflora*, SA1 for 0-1 cm from the root zone, SA2 for 1-3 cm from the root zone, SA3 for 3-5 cm from the root zone, SA4 for 5-10 cm from the root zone, SA5 for 10-17 cm.

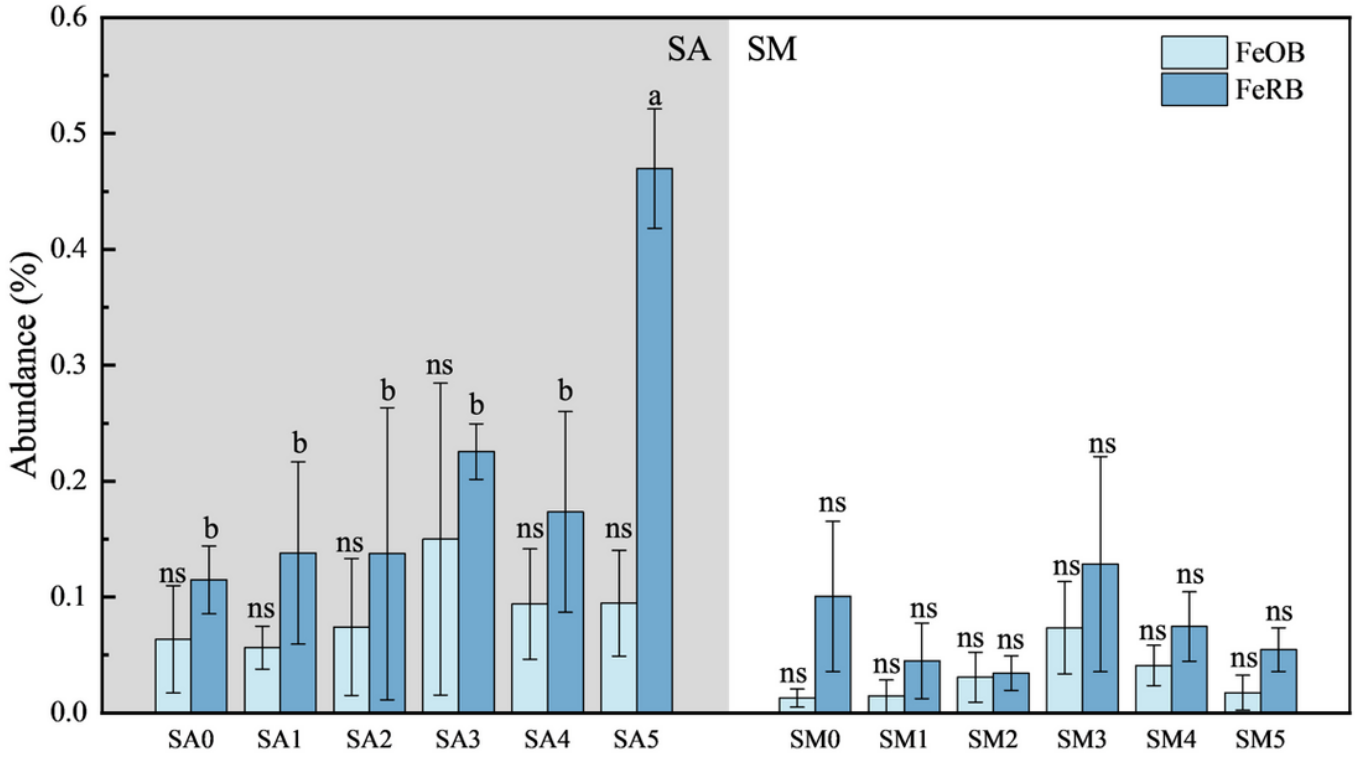


Figure 4

The relative abundance of the microbial Fe oxidation and reduction function in the soil of different distances from the root zone in the rhizoboxes of SA (*S. alterniflora*) and SM (*S. mariqueter*) predicted by the FAPROTAX database.

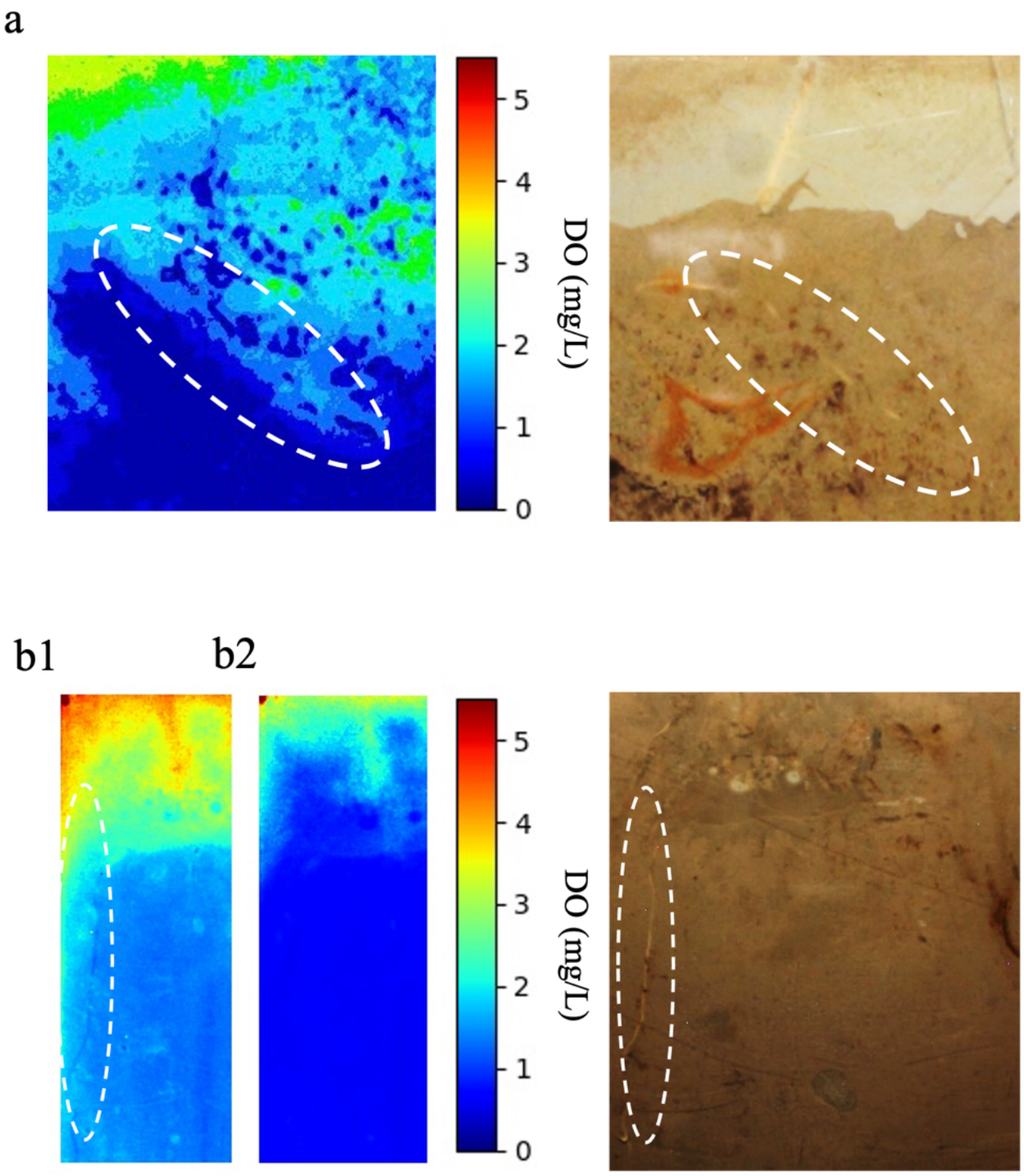


Figure 5

Oxygen distribution around the roots of *S. alterniflora*(a); Oxygen distribution around the roots of *S. mariqueter* when water was added to flood the soil (b1) and after stabilization for a while (b2). The circles represent the shape of roots.

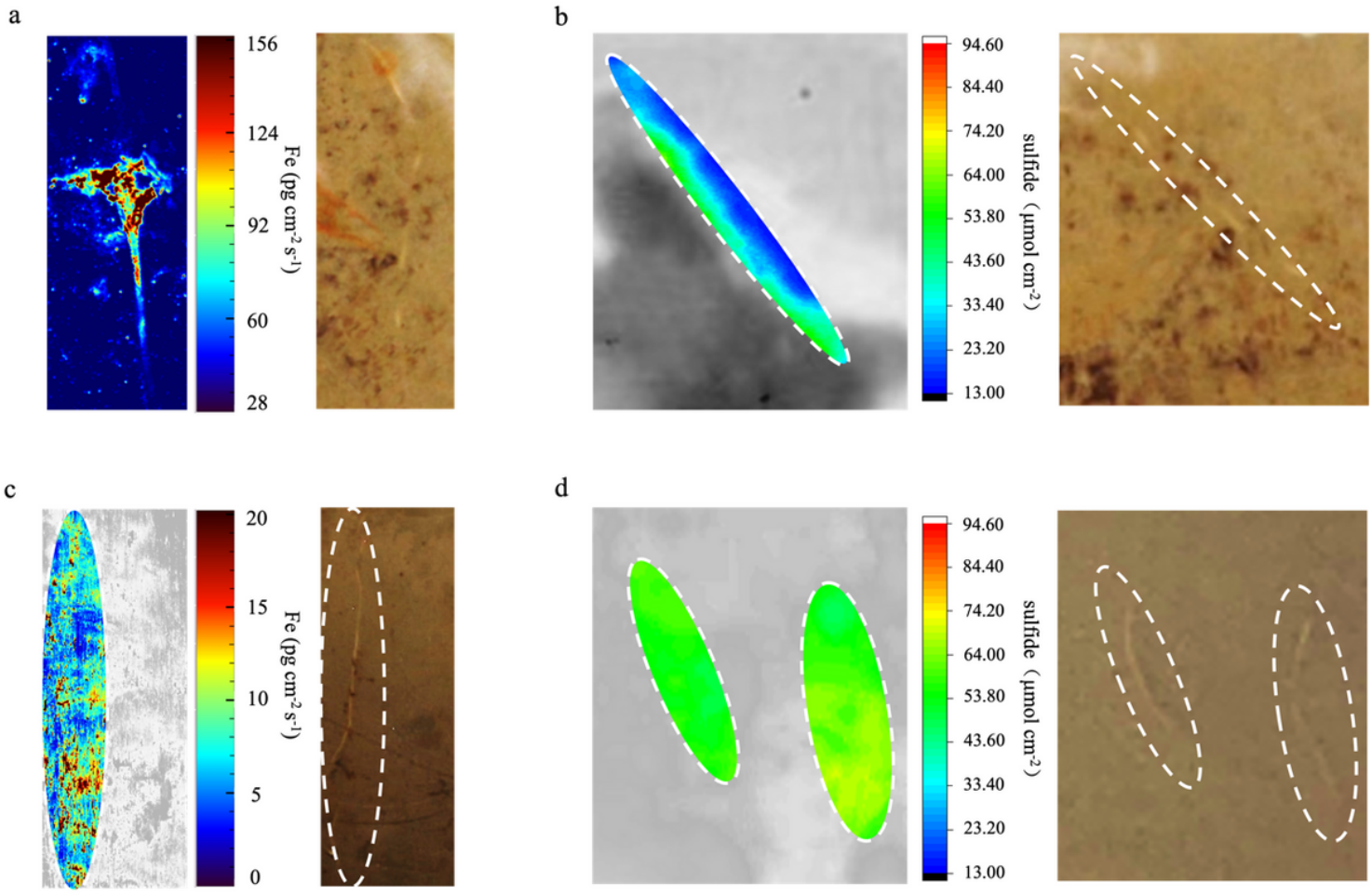


Figure 6

Iron distribution around the roots of *S. alterniflora*(a); Sulfide distribution around the roots of *S. alterniflora* (b); Iron distribution around the roots of *S. mariqueter* (c); Sulfide distribution around the roots of *S. mariqueter* (d). The circles represent the shape of the roots.

Supplementary Files

This is a list of supplementary files associated with this preprint. Click to download.

- Supplementaryfiles.docx